

**FILE COPY**

Circulate

File No. 28.304

**ANALYSIS OF WHITEWATER VALLEY UNIT 2  
ESP PROBLEMS DURING OPERATION OF THE  
LIFAC SO<sub>2</sub> CONTROL PROCESS**

Prepared for

Southern Company Services  
P.O. Box 2625  
Birmingham, AL 35202

SRI-ENV-93-650-7945-i

August 1993



**Southern Research Institute**



**Southern Research Institute**

August 31, 1993

Robert J. Evans  
Project Manager  
Clean Coal Technology  
U.S. Department of Energy  
Pittsburgh Energy Technology Center  
P.O. Box 10940  
Pittsburgh, PA 15236

Dear Bob:

Attached is a copy of Southern Research Institute's report to EPRI on the ESP problems during the LIFAC operation at Whitewater Valley. If you have any questions, please contact me.

Sincerely,

E. C. Landham, Jr.  
Head, Control Systems Technology Section

ECL/lcr

Report Distribution:

Ralph Altman, EPRI  
Dale Norris, RP&L  
Robert Evans, US/DOE  
James Hervol, ICF Kaiser Eng.  
Juhani Viiala, Tampella Power

**ANALYSIS OF WHITEWATER VALLEY UNIT 2 ESP PERFORMANCE  
PROBLEMS DURING OPERATION OF THE LIFAC SO<sub>2</sub> CONTROL PROCESS**

Prepared by

E. C. Landham, Jr.

**SOUTHERN RESEARCH INSTITUTE  
2000 Ninth Avenue South  
P. O. Box 55305  
Birmingham, AL 35255**

Prepared for

**ELECTRIC POWER RESEARCH INSTITUTE  
516 Franklin Building  
Chattanooga, TN 37411**

EPRI Contract RP3005-1

Dr. Ralph F. Altman  
Project Manager

August 1993

SRI-ENV-93-650-7945-i

## CONTENTS

1. INTRODUCTION .....	1
2. TEST RESULTS .....	3
PARTICLE MASS AND ESP PERFORMANCE .....	4
PARTICLE SIZE DISTRIBUTION .....	6
FLUE GAS SO <sub>x</sub> CONCENTRATIONS .....	7
DUST CHEMICAL COMPOSITION AND ELECTRICAL RESISTIVITY .....	9
ESP ELECTRICAL CHARACTERISTICS .....	12
FLY ASH TENSILE STRENGTH MEASUREMENTS .....	13
3. ESP PERFORMANCE MODELING .....	15
4. ANALYSIS AND RECOMMENDATIONS .....	19
5. REFERENCES .....	23

## 1. INTRODUCTION

The LIFAC flue gas desulfurization process is being demonstrated on Whitewater Valley Unit 2 of Richmond Power and Light. Although the LIFAC process has been successfully applied to several installations, problems have been encountered at Whitewater Valley with high stack opacity during LIFAC operation. Opacity excursions in excess of the 40% compliance limit occurred, and many tests have had to be aborted to maintain compliance. Southern Research Institute was contracted under EPRI RP3005-1 to assess the causes and suggest solutions to the opacity problems.

The LIFAC process uses calcium-based sorbent (limestone) injection into the furnace with a reactivation zone downstream of the air heater to combine the effects of both low and high temperature reactions between the calcium and flue gas  $\text{SO}_2$ . The reactivation occurs through cooling the flue gas to temperatures close to adiabatic saturation downstream of the air heater. The cooling is accomplished by spraying water into a large vertical conditioning chamber. Approximately 30 °F of steam reheat is used to provide a gas temperature of 170 °F to the downstream electrostatic precipitator (ESP). However, high stack opacity occurs at temperatures below about 200 °F, which has limited evaluation of the LIFAC process.

The ESP analysis program included field measurements to quantify several important aspects of the LIFAC/ESP system. Measurements were made both on the full-scale duct and in the EPRI Conditioning SideStream Pilot (CSSP) system, which allowed operation under conditions not possible with the full-scale system. Laboratory measurements of LIFAC dust properties were also made to support and enhance the field measurements. A mathematical computer model was used to analyze the actual performance of the ESP and to predict the performance levels which should result from the desired LIFAC operating conditions. The effects of several modifications to the ESP were evaluated with the model.

The next section of this report will present the results of the field and lab measurement program, providing appropriate analysis as needed. The third section will provide the results of the ESP modeling and upgrade projections, while the final section will provide analysis and recommendations.

## 2. TEST RESULTS

The program conducted at Whitewater Valley was designed to investigate the cause of the opacity problems and to suggest solutions. The most likely source was the ESP, but other possibilities were suggested, including the formation of sulfuric acid aerosol in the conditioning chamber or aerosol formation during combination of the gas streams of Units 1 and 2. The test program consisted of measurements of:

- ESP Inlet and Outlet EPA Method 17 mass trains, which include
  - Particle Mass Loadings
  - Gas Volume Flow
  - Gas Temperature
  - Gas Moisture
  - ESP Collection Efficiency
- ESP Inlet Particle Size Distributions
- Flue Gas Vapor Concentrations of SO<sub>2</sub> and SO<sub>3</sub>
- Dust Chemical Compositions
- In-Situ and Laboratory Dust Resistivity
- ESP Electrical Operating Conditions
- Stack Opacity

The measurements were made under 4 operating conditions to investigate different aspects of the process. The conditions are defined as follows:

Baseline	Normal, steady-state, fly ash only operation, no LIFAC.
Water Excursion	Measurements conducted during the first hour after startup of the humidification system with water flow of 37 gpm. No sorbent was added to the furnace.

**LIFAC Excursion**      Measurements conducted during the first hour after startup of the LIFAC process when the most serious opacity excursion occurred.

**LIFAC Post-Exc.**      After several hours of LIFAC operation and passing of the initial transient. This condition may be referred to as steady-state in other places in this report. Although that term might accurately describe the LIFAC system operation, true steady-state operation of the ESP would require a minimum of several days of continuous operation to achieve.

The measurement program was conducted over five days during the period April 5 - 9, 1993. The primary fuel burned during the tests was Black Beauty coal. In the following sections, the results of each of the major measurements will be presented and the implications to ESP performance discussed.

## **PARTICLE MASS AND ESP PERFORMANCE**

The results of the EPA Method 17 mass measurements at the ESP inlet and outlet are shown in Table 1 for the four test conditions. Measurements at the ESP inlet indicate that the addition of water to the flue gas had the expected effects of decreased temperature, decreased gas volume flow, and increased moisture content. Also as expected, both LIFAC tests produced an increase in inlet particle mass loading, in addition to the effects observed with water only. There were no significant differences between the excursion and post-excursion LIFAC periods.

However, the ESP outlet measurements and the ESP performance results shown in Table 2 indicate dramatic differences between the test conditions. Both excursion conditions increased ESP particle penetration (the percentage of particles which penetrate through

the ESP and escape) by a factor of 4 compared to the baseline conditions. The particle mass emission rate was increased more by the LIFAC excursion than with water only, but the difference is due to the increased inlet mass loading and not the collection performance of the ESP. The  $\omega_k$  parameter in Table 2 is the effective particle migration velocity calculated with the Matts-Ohinfeldt equation[1]. The  $\omega_k$  is an ESP collection performance indicator which is relatively insensitive to changes in ESP specific collection area (SCA) and inlet mass. The similarity of the  $\omega_k$  values for the two excursion conditions suggests that the ESP was affected in the same way by both water and LIFAC. After the initial excursion had subsided, the ESP collection performance with LIFAC returned to baseline levels, although particle emissions were still higher by the difference in inlet mass loading.

The opacity results in Table 2 show increases which generally correspond to the Unit 2 outlet mass emissions. However, since Unit 1 was on-line during the tests, the effects of the increased Unit 2 emissions were diluted by the Unit 1 gas stream prior to the opacity measurement location.

The conclusion drawn from the particle mass measurements is that significant increases in mass emissions from the ESP occurred during the startup transients. The transients did not appear to be a result of unexpected changes in the inlet conditions, but originated in the ESP. Water addition alone produced essentially the same transient effect on the ESP as did the LIFAC process, indicating that the effect was due to temperature and moisture and not related to the sorbent. The mass increases measured at the ESP outlet are more than sufficient to cause the increased opacity without any contribution from acid mists formed in the stack. After the transients passed, ESP performance improved. The appropriateness of the level of performance achieved with LIFAC will be investigated further in the section on ESP modeling.

Although acceptable ESP performance was obtained with LIFAC after the transient passed, the test conditions were 30-40°F above the desired operating temperature of

170°F. Several attempts were made to lower temperatures over a relatively short time period during the test program, each of which resulted in unacceptable opacity increases.

## PARTICLE SIZE DISTRIBUTION

The size distributions of the dusts entering the ESP were measured during the baseline and LIFAC steady-state conditions. The measurements were made in situ with modified Brink cascade impactors. The results are shown in Figures 1-3 as cumulative mass, cumulative percent mass, and differential mass distributions, respectively. On the cumulative graphs, each data point represents either the mass concentration or the percentage of the total mass contained in particles smaller than the indicated diameter. The differential distribution is the derivative of the cumulative mass distribution and illustrates the particle sizes where mass is concentrated, since the area under the curve in any size interval represents the amount of mass contained in that interval. The open circles on each plot indicate the results for the baseline fly ash, while the solid circles show the data with LIFAC. The error bars, most of which are smaller than the data symbol, represent 90% confidence intervals for the average distribution.

The shaded region on Figure 1 shows a typical particle size distribution for a bituminous coal ash from the EPRI database [2]. Comparison of the database and Whitewater Valley baseline distributions indicates that the baseline distribution is typical for the coal burned during the test program. Comparison of the baseline and LIFAC distributions indicates that the majority of the mass contributed by LIFAC was contained in particles larger than 1  $\mu\text{m}$ . Essentially no difference is observed between the baseline and LIFAC distributions below that size. This is in general agreement with furnace sorbent injection data from other sites.

## FLUE GAS SO<sub>x</sub> CONCENTRATIONS

The vapor-phase concentrations of SO<sub>2</sub> and SO<sub>3</sub> were measured at the outlet of the ESP during several of the test conditions. The measurements were made with the Cheney-Homolya modification [3] to the EPA Method 8 controlled-condensation sample train. The modification includes a heated quartz filter for removing fly ash from the gas stream. The filter is located between the sample probe and the SO<sub>3</sub> condenser and is heated to 550 °F to reduce reaction between the SO<sub>3</sub> vapor and the alkaline dust particles collected on the filter. The standard Method 8 technique utilizes a quartz wool plug in the end of the sample probe, which is at flue gas temperature where considerable reaction can occur. The modified technique is more accurate at low concentrations, and especially with unreacted sorbent present. A second useful characteristic of the Cheney-Homolya system for this application is that any suspended sulfuric acid droplets which have not reacted with the dust should be evaporated at the filter and show up as SO<sub>3</sub> vapor.

The results of the measurements are shown in Table 3 for baseline, water excursion, and LIFAC conditions. Since the actual levels of SO<sub>3</sub> in the gas stream are of interest here, the concentrations have not been normalized to a common oxygen concentration. Excluding the low value of 2.59, which was at a very high O<sub>2</sub> level and low temperature, an average baseline SO<sub>3</sub> value of 4.8 ppm is obtained. Using the average baseline SO<sub>2</sub> value of 1737 ppm, an effective SO<sub>2</sub> to SO<sub>3</sub> conversion rate of 0.3% is calculated, which is fairly typical for an Eastern bituminous coal. Thus, the baseline conditions were generally unremarkable.

When water addition was used to cool the flue gas, most of the SO<sub>3</sub> was lost prior to the ESP outlet measurement location. The missing SO<sub>3</sub> vapor was either adsorbed on the fly ash particles because of the lower temperature or condensed in the conditioning chamber. Since the sampling system would evaporate sulfuric acid droplets, the low concentration levels measured indicate that if such droplets were created by

condensation and nucleation, they were collected in the ESP and would not contribute to an opacity problem.

During LIFAC operation, the measured  $\text{SO}_3$  concentrations were at or below the detection limit of 0.3 ppm. Essentially complete uptake of the  $\text{SO}_3$  is typical of the dry  $\text{SO}_2$  control processes which we have studied. Once again there is no indication that sulfuric acid droplets are contributing to an opacity plume.

If the assumption that sulfuric acid droplets would be evaporated by the sampling system is incorrect, the  $\text{SO}_3$  measurement would not correctly indicate the presence of droplets, as assumed above. However, the mass which would be contributed to total particle emissions from the condensation of acid vapor can be calculated from the measured  $\text{SO}_3$  concentrations. If the entire baseline concentration of 5 ppm of  $\text{SO}_3$  vapor were to condense to  $\text{H}_2\text{SO}_4$  droplets, it could have significant effect on opacity, but would correspond to a mass emission rate of only  $0.02 \text{ lb}/10^6 \text{ Btu}$ . This potential mass concentration increase is almost an order of magnitude less than that measured by the mass trains during the excursions. Therefore, the condensation of sulfuric acid droplets cannot account for the increased ESP outlet mass.

An additional argument against a sulfuric acid plume is the temporary nature of the opacity excursion. If sulfuric acid condensation were responsible for the opacity excursions, there is no reason for the transient to pass and for the opacity to clear with time. Considering all of the data, any significant effect of condensed acid from Unit 2 on the opacity problems can be dismissed.

Measurements of the  $\text{SO}_3$  concentrations in the flue gas from Unit 1 revealed values which ranged from 6 to 8 ppm, which are slightly higher, but generally in agreement with the Unit 2 data. Although we cannot unequivocally say that condensation of acid droplets from the combination of the gases from the two units is not contributing to opacity, we do not believe this to be a significant problem. Again, there is sufficient particle mass

emitted from Unit 2 to account for the entire problem and there is no reason for a condensation problem to clear up with time.

## DUST CHEMICAL COMPOSITION AND ELECTRICAL RESISTIVITY

The chemical compositions of dusts collected from the ESP hoppers during the baseline and LIFAC tests are shown in Table 4. Because of the short time for equilibration of the ESP, the suitability of the LIFAC samples may be questionable, particularly the outlet field sample. That is, the concentration of sorbent in these samples may be lower than will be encountered during long-term operation. Regardless, the LIFAC samples indicate the expected trends of large increases in the calcium and soluble sulfate contents and dilution of most other components. The moderately increased B.E.T. surface area of the LIFAC dust is typical of limestone furnace addition processes.

The electrical resistivity of the dust is generally one of the most important factors controlling ESP performance. Ideal resistivity levels occur from about  $5 \times 10^9$  to  $2 \times 10^{10}$  ohm-cm, a range where the resistivity is sufficiently low that ESP electrical conditions are not significantly limited, but high enough that electrical clamping forces are adequate to hold collected dust on the ESP electrodes. The resistivity of the dust is a function of its chemical composition, temperature, moisture, and  $\text{SO}_3$  vapor concentration. Bickelhaupt has developed a predictive technique [4,5] for fly ash resistivity which illustrates the effects of the changes in composition observed in the Whitewater Valley dust. Figures 4 and 5 show the predicted resistivity as a function of temperature for the inlet hopper samples of Table 4. On each graph, the resistivity trend is calculated for four  $\text{SO}_3$  concentrations: 1 ppm, 4 ppm, 10 ppm, and the value measured during the test. The model predicts that the baseline fly ash (Figure 4) should have resistivity values in the range of  $1 \times 10^{10}$  to  $1 \times 10^{11}$  ohm-cm under the conditions of the test (300-330° F, 3-5 ppm  $\text{SO}_3$ ).

The resistivity prediction for the LIFAC samples indicates a significant shift in the peak of the resistivity curve, producing lower values in the low-temperature range of interest with no SO<sub>3</sub> present. However, this model was developed for fly ash and sometimes has not compared well with other measurement techniques on sorbent/ash mixtures, so this result should be treated with caution.

Measurements of resistivity were made in the laboratory in a simulated flue gas environment for the samples of Table 4. The measurements were made generally in accordance with IEEE 548-1984 in both the ascending and descending temperature modes. The measurement deviated from the standard measurement technique in that the maximum temperature was limited to 550 °F rather than the prescribed temperature of 850 °F. This lower limit is usually used on sorbent containing dusts to prevent chemical changes in the sample. The results of the measurements are shown in Figure 6. The two fly ash samples gave essentially identical results and were not affected by the temperature mode. The two LIFAC samples, on the other hand, gave quite different results depending on the calcium content of the sample and the temperature mode. The LIFAC resistivity values ranged over two orders of magnitude in the temperature range of interest (170-200 °F). Because of a limited database with sorbent/ash mixtures and LIFAC in particular, we cannot say whether the ascending or descending data more accurately reflect the conditions in the ESP inlet duct. Therefore, we will treat the lab data as a range of possible values.

Resistivity measurements were made in situ during the test program with a point-plane resistivity probe. Measurements were made in the main ESP inlet duct during baseline and LIFAC operating conditions down to the temperatures that could be safely operated without exceeding allowable stack opacity. Resistivity measurements were also made in the EPRI Conditioning SideStream Pilot system so that the water injection capability of that system could be utilized to lower the gas temperature to levels below those possible in the main duct. The in-situ resistivity data obtained are tabulated in Table 5. At first glance, the lack of change in resistivity values as temperature drops from the baseline

(>300°F) to LIFAC (<200°F) conditions seems confusing until one considers that the drop in temperature is accompanied by the loss of the SO<sub>3</sub> vapor. Figure 7 compares the in-situ data to appropriate lab and predicted data. On the figure, the open circles are the predicted resistivity data for the baseline fly ash while the shaded area represents the upper and lower limits of the lab measurements with no SO<sub>3</sub> present. Compared to these data, the solid symbols representing the in-situ data are understandable. The trend of the baseline in-situ data (triangles) follow the predicted acid slope and lie between the predicted values for 1 and 4 ppm. The LIFAC in-situ data (boxes) are almost completely enclosed in the area of the lab measurements with no SO<sub>3</sub> present. Given the limits of the techniques, this would have to be considered good agreement.

In summary, the baseline data indicate acceptably low resistivity most of which should not significantly limit ESP performance. Most of the data obtained indicated that the resistivity was  $5 \times 10^{10}$  ohm-cm or less. On 4/7/93, with a temperature above 325 °F, resistivity values as high as  $1 \times 10^{11}$  ohm-cm were observed, which would begin to limit ESP performance more severely. With LIFAC, the resistivity ranged from the low  $10^{10}$  to the mid  $10^9$  ohm-cm range. Very good ESP electrical conditions should result from these values and collection should be excellent. However, the reduction in resistivity will reduce the electrical holding force keeping the collected dust on the electrodes. This effect will be discussed in more detail later.

It should be noted that during most of the baseline resistivity tests (and the baseline ESP performance tests) the flue gas was passed through the LIFAC conditioning chamber. This was done to keep the conditions which were not being evaluated as constant as possible between the tests. Although no water was added, some cooling of the gas did occur in the chamber because of the extra duct surface. Therefore, the baseline resistivity of the fly ash and the collection performance of the ESP may have been somewhat better than normally experienced on this unit.

In addition to the problems during operation of the LIFAC process, problems have also been encountered with high opacities which occur after shutting down LIFAC after extended periods of operation. The reason for this is evident from the data in Figure 7, which shows that the LIFAC dust can have resistivity values up to  $10^{13}$  ohm-cm at 300 °F, if no  $\text{SO}_3$  is present. When LIFAC is first turned off, the ESP electrodes are coated with substantial quantities of LIFAC dust which will take hours or days to completely replace with fly ash. When the water addition stops, the temperature increases rapidly, increasing the resistivity of the ash/sorbent dust layer, and thereby degrading ESP electrical conditions and collection performance. The LIFAC dust is susceptible to conditioning with  $\text{SO}_3$ , but with only 5 ppm naturally available, the large quantities of unreacted sorbent will take substantial time to condition. The best solution to this problem is to use water addition to reduce the resistivity during this shutdown transient period. No more water than necessary should be used and for no longer than necessary to limit the potential for corrosion as free  $\text{SO}_3$  becomes available.

## ESP ELECTRICAL CHARACTERISTICS

The ESP electrical conditions measured during each of the major test periods are shown in Table 6. As expected from the resistivity data, the electrical conditions do not indicate a substantial limitation because of the collected dust layer under any conditions. During baseline operation, the current densities were in the range of 17 to 23 nA/cm<sup>2</sup>, which are generally consistent with resistivity around the mid  $10^{10}$  ohm-cm. During all of the low temperature tests (water addition or LIFAC), the ESP electrical conditions improved slightly over the baseline case suggesting a reduction in resistivity. Greater increases in current density would probably have occurred at low temperature, but the ESP power supplies were at their current output limit of 25 nA/cm<sup>2</sup>. Figure 8 shows voltage-current density curves for three fields of the ESP during LIFAC. The outlet field was not measured to keep opacity excursions to a minimum. The electrical characteristics show

no anomalous conditions, such as back corona, and indicate that all of the power input to the ESP was useful for charging and collecting particles.

Because of the interelectrode space charge created by electrically-charged, suspended particles, the highest voltages should be seen in the inlet field of the ESP with decreasing values toward the outlet. The low values in the inlet fields could be caused by electrode misalignment or by incorrect meter calibrations. The EPRI database of ESP electrical conditions [2] indicates that this ESP would be expected to operate at voltages of 54.2, 50.3, 47.7, and 48.4 kV for fields 1 through 4, respectively, at a current density of 25 nA/cm<sup>2</sup>. Except for the outlet field, the database values are much higher than the measured voltages (for the same current density) and would result in significantly better performance. If the meters are out of calibration and are reading low there is no operating penalty, but the ESP modeling results discussed in a subsequent section will be adversely affected.

## FLY ASH TENSILE STRENGTH MEASUREMENTS

The tensile strength of the fly ash and LIFAC dust samples was measured using an electrostatic tensiometer. This device determines the magnitude of the attractive forces between particles in a dust layer. The measurement is made at room temperature, but the relative humidity is controlled to simulate the flue gas environment. There is no current through the dust layer during the measurement, so the electrical clamping force, which is a function of the current and resistivity of the layer, is not included. The measurements were made at two relative humidity levels (12 and 23%), which bracket the conditions observed during the LIFAC test program. The measurements (Table 7) indicate:

1. The tensile strength of both dusts were reduced as relative humidity increased from 12% to 23%. This is consistent with most of the dusts tested with this

device which have exhibited a minimum in tensile strength between 34% and 50% RH.

2. The outlet hopper samples had much higher tensile strengths than did the inlet hoppers. This is probably related to the finer size distribution in the outlet hoppers and the higher adhesion properties of small particles.
3. The tensile strength of the LIFAC dust was greater than that of the fly ash for both humidity levels.

The absolute values of the tensile strength of the Whitewater Valley dusts were not unusual, but fell in the middle of the range of other fly ashes and ash/sorbent mixtures. The reduction in tensile strength with increasing relative humidity may be significant to the performance problems and will be discussed later.

### 3. ESP PERFORMANCE MODELING

Version 3 of the SRI Mathematical Model of ESP Performance [6] was used to simulate the Whitewater Valley Unit 2 ESP under a variety of conditions. The model was used for comparison with the measured ESP performance, to predict the performance of the ESP under the desired LIFAC operating conditions, and to make projections of the effect of several ESP modifications on both fly ash and LIFAC performance. The hardware specifications of the existing ESP used in the model are shown in Table 8. The measured flue gas and particle characteristics were used in the model, as were the measured ESP electrical conditions. Two different parameters which describe non-ideal conditions inside the ESP are used to adjust the model to account for sneakage and reentrainment ( $s$ ) and the uniformity of the gas flow distribution ( $\sigma_g$ ). Sneakage describes the particles which bypass each electrified section of the ESP by flowing through hoppers and over the tops of plates, while reentrainment accounts for particles which are collected, but subsequently reentrain into the gas stream. The  $\sigma_g$  parameter is the coefficient of variation of the gas velocity profile in the ESP. For ESPs collecting fly ash, values of  $s$  and  $\sigma_g$  of 0.05 and 0.15 have been shown to correspond to modern ESPs in good condition, while older ESPs in questionable condition are better described by values of 0.10 and 0.25 [2]. For each test condition, both sets of model non-ideal conditions were used to estimate a range of expected performance.

The model calculations of ESP performance for the four conditions evaluated during the test program are shown in the top half of Table 9a, while Figure 9 compares the model calculations to the measured ESP performance on a particle emissions basis. In the figure, the leftmost two bars of each group show the model computed performance with the two sets of non-ideal conditions, while the rightmost (black) bar shows the measured performance. The groups of bars correspond to the different test conditions. As shown by the leftmost group of bars, the measured baseline performance of the Unit 2 ESP was somewhat better than the model predictions with both sets of non-ideal conditions. This is surprising considering some of the problems with this ESP. However, if the model is

run using the voltages predicted by the EPRI database for the Unit 2 current densities, the predicted performance is much better, and the measured performance corresponds better to expectations. Regardless of the reason for the disagreement, observing relative changes in the measured and model computed performance will illustrate the issues here.

When the model predictions are compared to the measured results under the two excursion conditions, the model greatly overpredicts performance. In both excursion cases, the model predicted improved performance and reduced emissions compared to the baseline case. The theoretical improvement in performance occurs at low temperature because of the improved electrical conditions and reduced gas volume flow. The reduction in emissions should occur despite the higher inlet mass loading during the LIFAC excursion. In real life, however, the particle emissions from the ESP dramatically increased. Obviously, there is some mechanism at work which has not been taken into account in the model. With the LIFAC steady-state condition, the model corresponds better to the measured performance, but the relationship between measured and model values has still shifted relative to the baseline case. That is, during all of the low temperature tests, there appears to have been a change in the non-ideal conditions in the ESP which has not been accounted for by the model.

The symbols on Figure 10 show the performance of a number of ESPs operating downstream of spray dryers. Spray dryers produce conditions in a ESP similar to those associated with LIFAC. The unshaded bounded area on the graph indicates the range of model predictions using the standard non-ideal conditions derived for fly ash (0.05, 0.15 and 0.10, 0.25) and which were used in the model runs discussed above. Except when calcium chloride was used to make the dust sticky, the measured performance of all the ESPs is much worse than the model predictions. The shaded area on the figure shows ESP model predictions using non-ideal conditions of 0.25, 0.25 (lower limit) and 0.50, 0.25 (upper limit). Most of the data points are encompassed by this area. The change in non-ideal conditions is probably related to reentrainment of previously collected particles. This assertion is strongly supported by the Shawnee data with and without

calcium chloride addition. The mechanisms of increased particle reentrainment will be further discussed in a later section.

When non-ideal conditions of 0.25, 0.25 and 0.50, 0.25 are used to model LIFAC operation with the existing Whitewater Valley Unit 2 ESP, the performance indicated in the bottom half of Table 9a and by the leftmost group of bars on Figures 11 and 12 is obtained. Particle emissions are predicted to be between 0.19 and 0.77 lb/10<sup>6</sup> Btu, and the opacity range is 25 to 57%. These levels are much worse than those measured during the test program, but this is reasonable since they represent operation at 170° F. The opacity values assume that Unit 1 is off line and that only Unit 2 contributes to the stack appearance. If Unit 1 were operating without serious problems, some dilution of the mass concentration would occur to reduce the higher opacity levels. The reduction in opacity with both units on line would be roughly equal to the ratio of the products of each unit's opacity and gas flow. This range of stack opacity is marginal with respect to compliance. That is, based on the model projections, the existing ESP may or may not operate in an acceptable range.

One factor which is working against the Unit 2 ESP with LIFAC is very high gas velocities in the bottom of the ESP. Figure 13 shows the gas velocity profile measured at the inlet of the ESP by EPSCON [7]. With an average gas velocity of 6.9 ft/sec, there were many locations in the bottom half of the ESP which exceeded 10 ft/sec and a significant number over 15 ft/sec. Design gas velocities for modern ESPs are in the range of 3.5 ft/sec and values in excess of 5 ft/sec can degrade ESP performance by causing excessive particle reentrainment. The high velocities can increase the magnitude of rapping puffs and actually scour particles from the surface of collected dust layers. Although the ESP model has a non-ideal parameter for gas flow distribution, this parameter does not account for increased reentrainment from excessive velocity. Considering the gas distribution in the Unit 2 ESP, the LIFAC model projections may be optimistic.

The effect on LIFAC performance of increasing the size of the Unit 2 ESP was also estimated with the ESP model. Three modifications were considered, all of which include increasing the collecting plate height from 30 to 40 feet. The plate height increase is considered necessary to increase the ESP cross-sectional area and to reduce the gas velocities. The first option was with that change only, while the other two included adding either one or two 7.5 ft long collecting sections to the outlet of the ESP. The hardware specifications of the modified ESP configurations are provided in Table 10, while the model predictions are shown in Table 9b and in Figures 11 and 12. The model indicates that two additional fields would be required to ensure that opacity remains below 30% with LIFAC when Unit 1 is off line.

Projections of the performance of the modified ESP were also made with two different fly ashes and are shown in Table 9b. Figures 13 and 14 show the model projections for the baseline fly ash and Figures 15 and 15 provide the results with a very high resistivity dust. The resistivity for the second case was assumed to be  $1 \times 10^{12}$  ohm-cm, and the ESP electrical conditions were predicted from the EPRI database. The figures indicate that the addition of two fields to the ESP should produce very good performance with most ashes likely to be encountered.

#### 4. ANALYSIS AND RECOMMENDATIONS

The measurement program established that the source of, at the least, the majority of the opacity excursion observed during LIFAC startup is related to emission of particles from the ESP. Even when only water addition was used to drop the gas temperature with no change in ESP inlet mass or particle size distribution, large increases in ESP emissions occurred. Even if all of the SO<sub>3</sub> in the gas stream was condensed to sulfuric acid droplets, which were collected in the sample train, that could account for only 10-20% of the observed increase in mass.

The electrical operating conditions of the ESP were very good during the LIFAC tests indicating that high dust resistivity was not limiting the performance of the ESP. There was no indication that the excursions occurred because the fundamental collection performance of the ESP was degraded. Therefore, the source of the excursion appears to be a release of dust which has previously collected in the ESP. In fact, the vast majority of the dust emitted during the initial excursion must be fly ash rather than LIFAC dust. There are tens of thousands of pounds of dust residing on the ESP plates at any time, and the release of only a small quantity of this dust would be required to create the excursions observed.

The low temperature, high humidity conditions generated by LIFAC tend to reduce the forces which hold the collected dust layer on the ESP electrodes through two avenues. First, the dust resistivity is reduced which reduces the electrical clamping force. This force is a function of the dust resistivity and the corona current through the dust layer. At Whitewater Valley, the current density was increased only slightly (from 20 to 25 nA/cm<sup>2</sup>), while in-situ dust resistivity was reduced by an order of magnitude or more to 5x10<sup>9</sup> ohm-cm (in-situ) or 5x10<sup>8</sup> ohm-cm (Lab). This should result in a 2 to 3 order of magnitude drop in the electrical holding force [8]. The second mechanism for reduction in holding force is the reduction in tensile strength of the dust. The increase in relative

humidity from 12 to 23% decreased the tensile strength of the inlet samples by 25% and the outlet samples by more than 50%.

Therefore, it appears that the most likely cause of the high opacity excursions is a combination of reduced holding force and the high gas velocities in the ESP producing reentrainment of previously collected dust. During baseline operation, stable dust layers are created which balance the electrical and adhesive holding forces against the shearing forces of the gas flow. When the conditions are suddenly changed to low temperature and high humidity, the reduced electrical and tensile forces result in removal of dust from the electrodes until a new stable (thinner) dust layer is reached. This problem could be expected to reoccur if the conditions change again to increase relative humidity. The small size, high gas velocities, and low current limit of the Whitewater Valley Unit 2 ESP make this problem much more obvious than it might be in other situations.

The steady-state operation of the ESP during LIFAC will also be affected by the reduced holding forces. Reduced holding force is a likely cause of the higher reentrainment correction which must be used in the ESP model with most of the low-temperature sorbent processes we have observed. The magnitude of the steady-state LIFAC reentrainment problem has not yet been determined at Whitewater Valley. We recommend that additional attempts to operate the ESP with LIFAC at 170°F and no bypass should be made during long-term tests with plenty of time allowed for transient conditions to pass when changes are made. This could be accomplished by reducing bypass until opacity increases, maintaining that setting until the transient passes, then further reducing bypass until opacity increases again. This process should be iterated until the bypass is closed or no further reductions in bypass can be made without unacceptable opacity increases. At a minimum, several hours should be allowed for each transient to pass before determining that no additional changes can be made.

Since both of the mechanisms which hold the dust on the collecting electrode are inversely related to relative humidity, decreasing the relative humidity should reduce

particle reentrainment and improve ESP operation with LIFAC. Figure 17 shows the relationship between relative humidity and gas temperature for several moisture levels. During the test program, acceptable ESP performance was measured at 196°F and 12.2% moisture, which corresponds to about 17% relative humidity. At the desired LIFAC operating condition of 170°F and 13.5% moisture, the relative humidity increases to 33% because of the increased water and decreased temperature. Increasing the ESP temperature to 205°F by using additional reheat would compensate for the higher moisture content and provide approximately the same humidity as during the test program. In our opinion, this is likely to result in improved performance.

From an economic standpoint, the cheapest source of heat in a coal-fired power plant is hot flue gas. It is therefore logical to use this source of heat to obtain the additional reheat necessary to reduce flue gas relative humidity and improve ESP performance. We suggest bypassing a fraction of high-temperature flue gas around the air heater and recombining it with the cool gas at the outlet of the LIFAC conditioning chamber. The gas volume required would depend on the temperature of the hot gas. A major concern in the design of such a system should be achieving good distribution of the hot gas to avoid serious temperature gradients in the ESP which could degrade performance.

The poor gas flow distribution and high gas velocities in the ESP are certainly contributing to reduced ESP performance under baseline conditions, but especially during LIFAC. Durham has shown that increasing the ESP gas velocity from 3.6 to 4.1 ft/sec with a low-temperature sorbent process increased particle penetration by a factor of 1.76 [10]. With the E-SO<sub>x</sub> process operating at 170°F on an ESP with SCA of 250 ft<sup>2</sup>/1000 acfm, Marchant measured a collection efficiency of 96% when flow distribution problems produced gas velocities of 10 ft/sec in the bottom of the ESP [11]. The Whitewater Valley ESP gas velocities of 10-15 ft/sec in the bottom of the ESP are believed to be largely responsible for the poor performance. Unfortunately, we do not currently have a technique for estimating the actual effect of high gas velocities on ESP emissions. However, the evidence strongly indicates that improving the distribution will improve

performance, and we recommend that a flow study be performed and changes be made to the flow distribution devices.

Although an increase in non-ideal conditions apparently occurs with all ESPs on low-temperature sorbent processes, large, well designed ESPs with low gas velocities do not appear to have serious particle emissions problems at 170°F [9]. The ESP model indicates that increasing the plate height and adding two additional 7.5 ft. long fields to the Whitewater Valley 2 ESP should result in acceptable performance with LIFAC. These modifications would also provide excellent performance with essentially any fly ash encountered in the future.

In summary, the following recommendations are made to evaluate and improve the operation of the Whitewater Valley Unit 2 ESP during LIFAC:

1. Separate the excursion conditions from steady-state operation more clearly to determine the extent of the steady-state reentrainment problem. Determine if the ESP can operate at the design operating conditions if ESP temperature is decreased gradually over a period of days with plenty of time for transient conditions to pass.
2. Increase the amount of reheat to keep relative humidity in the range where acceptable ESP performance is achieved.
3. Conduct a gas flow study and make modifications to improve the gas flow distribution in the ESP as much as practical.
4. If the preceding items do not result in acceptable performance, increasing the ESP plate height to 40 ft and adding an additional 15 ft of collecting length to the ESP should produce compliance performance.

## 5. REFERENCES

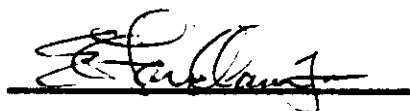
1. S. Matts and P. O. Ohnfeldt, "Efficient Gas Cleaning with SF Electrostatic Precipitators". AB Svenska Flaktfabriken Technical Bulletin, 1973.
2. J. L. DuBard and R. S. Dahlin. Precipitator Performance Estimation Procedure. Electric Power Research Institute. Palo Alto, California. EPRI CS-5040. February 1987.
3. Cheney, J. L. and J. B. Homolva, "Sampling Parameters for Sulfate Measurements and Characterization," Environ. Sci. & Technology, 13(5) 584-588, 1979.
4. R. E. Bickelhaupt. A Technique for Predicting Fly Ash Resistivity. U. S. Environmental Protection Agency. Research Triangle Park, North Carolina. EPA-600/7-79-204. July 1979.
5. R. E. Bickelhaupt. A Study to Improve a Technique for Predicting Fly Ash Resistivity with Emphasis on the Effect of Sulfur Trioxide. U. S. Environmental Protection Agency, Research Triangle Park, NC. EPA Report Number 600/7-86/010. NTIS PB86-178126. 1986.
6. M. G. Faulkner and J. L. DuBard. A Mathematical Model of Electrostatic Precipitation (Revision 3): Vol. I. U. S. Environmental Protection Agency. Research Triangle Park, North Carolina. EPA-600/7-84-069. July 1984.
7. "Measurement of Gas Velocity and Flow Distributions in the Richmond Department of Power and Light Whitewater Valley Station Unit 2 Electrostatic Precipitator on May 20, 1992. Report to Richmond Power and Light by EPSCON-FLS, Inc.
8. D. H. Pontius and T. R. Snyder, "Measurement of the Tensile Strength of Uncompacted Dust Aggregates", Powder Technology, vol 68, p159-162, 1991.
9. E. C. Landham, Jr., K. M. Cushing, Ralph F. Altman, Brian D. Larson, John B Doyle. "Effects of Spray Dryer Effluent on the Performance of the Laramie River Unit 3 ESP". in Proceedings: Ninth Symposium on the Transfer and Utilization of Particulate Control Technology. Electric Power Research Institute, Palo Alto, CA. 1991.
10. M. D. Durham, et al. "Low-Resistivity Related ESP Performance Problems in Dry Scrubbing Applications". Journal of Air and Waste Management Association, Vol. 40, No. 1, January 1990.

11. G. H. Marchant, et al. "Effects of E-SO<sub>x</sub> Technology on ESP Performance". Final Report, EPA Cooperative Agreement No CR-814915-01-0. U.S. Environmental Protection Agency, Research Triangle Park, NC. May 1992.

Submitted by:

E. C. Landham, Jr.

Head, Control Systems Technology Section

A handwritten signature in black ink, appearing to read "E. C. Landham, Jr.", written over a horizontal line.

Approved by:

D. H. Pontius

Director, Particulate Sciences Research

A handwritten signature in black ink, appearing to read "D. H. Pontius", written over a horizontal line.

TABLE 1. Whitewater Valley Unit 2 Particle Mass Data

Test Condition	Particle Mass		Gas Flow, acfm	Gas Temp., °F	Gas Moisture, %	Gas Oxygen, %
	gr/acf	lb/10 <sup>6</sup> Btu				
ESP Inlet						
Baseline	1.61	5.16	247,600	307	7.9	5.6
Water Excursion	1.66	5.01	230,400	224	11.4	5.7
LIFAC Excursion	3.25	9.18	227,800	210	10.8	5.7
LIFAC Post-Exc	3.22	8.71	216,800	196	11.0	5.3
ESP Outlet						
Baseline	0.0158	0.0490	243,400	307	8.1	5.5
Water Excursion	0.0703	0.2192	250,700	279	11.8	5.5
LIFAC Excursion	0.1239	0.3621	235,700	231	13.6	5.2
LIFAC Post-Exc	0.0248	0.0701	220,900	212	13.3	5.2

TABLE 2. Whitewater Valley Unit 2 ESP Performance Results

Condition	ESP Efficiency, %	ESP Penetration, %	Particle Emissions, lb/10 <sup>6</sup> Btu	ESP <sup>a</sup> $\omega_k$ , cm/sec	ESP SCA, ft <sup>2</sup> /kacfm	Stack <sup>b</sup> Opacity, %
Baseline	99.050	0.950	0.0490	62	182	10
Water Excursion	95.625	4.375	0.2192	26	195	22
LIFAC Excursion	96.056	3.944	0.3621	27	198	24
LIFAC Post-Exc.	99.195	0.805	0.0701	58	208	13

a. Effective Migration Velocity from Matts-Ohlnefeldt Equation with k=0.5  
b. Measured in Stack with Both Units On-Line.

TABLE 3. Whitewater Valley Unit 2 SO<sub>x</sub> Results

Test Condition	Gas Temperature, °F	Vapor Concentration, ppmv <sup>a</sup>		Oxygen Content, %
		SO <sub>2</sub>	SO <sub>3</sub>	
Baseline	306	1739	5.43	5.6
	308	1723	5.53	5.6
	311	1726	5.61	5.5
	307	1749	4.42	5.0
	307	1685	3.91	5.6
	299	1539	2.59	7.7
	302	1800	4.02	5.6
Water Excursion	249	1752	0.78	5.6
	234	1778	0.66	5.6
LIFAC	238	1509	0.37	5.6
	223	1539	0.31	5.3
	211	1636	<0.3	5.1
	210	1637	<0.3	5.2

a. Actual duct concentration - not normalized for oxygen content.

TABLE 4. Chemical Composition of ESP Hopper Samples  
(Weight %)

	Fly Ash		LIFAC Dust	
	Inlet Hopper	Outlet Hopper	Inlet Hopper	Outlet Hopper
Li <sub>2</sub> O	0.03	0.04	0.02	0.02
Na <sub>2</sub> O	0.62	0.79	0.55	0.45
K <sub>2</sub> O	2.3	2.5	1.7	2.2
MgO	0.91	0.95	0.90	0.99
CaO	2.6	2.4	32.3	21.6
Fe <sub>2</sub> O <sub>3</sub>	21.7	20.7	13.3	13.5
Al <sub>2</sub> O <sub>3</sub>	22.2	23.4	14.8	19.8
SiO <sub>2</sub>	48.9	47.6	32.3	37.3
TiO <sub>2</sub>	1.1	1.2	0.74	0.91
P <sub>2</sub> O <sub>5</sub>	0.42	0.54	0.22	0.34
SO <sub>3</sub>	0.58	0.51	4.6	4.6
LOI	3.8	5.4	5.0	4.4
Soluble SO <sub>4</sub> <sup>-2</sup>	1.0	1.4	5.6	5.0
B.E.T., m <sup>2</sup> /g	1.2	1.9	4.1	3.4
Equil. pH	8.8	8.2	11.1	10.9

TABLE 5. In-Situ Resistivity Data

Test Location	Date	Test Condition	Gas Temperature, °F	Spark Resistivity, ohm-cm
Main Duct	4/5/93	Baseline	311	$2.76 \times 10^{10}$
			312	$3.08 \times 10^{10}$
			311	$2.32 \times 10^{10}$
	4/6/93	LIFAC	218	$2.97 \times 10^{10}$
			208	$1.84 \times 10^{10}$
			200	$3.07 \times 10^9$
			190	$7.54 \times 10^9$
			193	$1.49 \times 10^{10}$
			194	$1.66 \times 10^{10}$
	4/7/93	Baseline	326	$1.75 \times 10^{11}$
			329	$1.20 \times 10^{11}$
			329	$5.40 \times 10^{10}$
CSSP	4/8/93	Baseline	298	$2.26 \times 10^{10}$
			298	$2.13 \times 10^{10}$
		LIFAC	203	$5.99 \times 10^{10}$
			200	$4.91 \times 10^{10}$
			201	$5.54 \times 10^{10}$
		LIFAC + H <sub>2</sub> O	167	$8.27 \times 10^9$
	170		$6.81 \times 10^9$	
	4/9/93	Baseline	299	$5.15 \times 10^{10}$
			293	$1.59 \times 10^{10}$
		LIFAC	196	$3.77 \times 10^{10}$
LIFAC + H <sub>2</sub> O		146	$4.23 \times 10^9$	
	171	$< 5 \times 10^9$		
		171	$1.90 \times 10^{10}$	

**TABLE 6. Whitewater Valley 2 ESP Electrical Conditions**

Condition	ESP Field	Voltage, kV	Current, mA	Current Density, nA/cm <sup>2</sup>
Baseline	1	42.7	193	18.5
	2	43.4	180	17.3
	3	47.1	203	19.5
	4	49.7	240	23.0
Water Excursion	1	43.4	265	25.4
	2	43.4	260	25.0
	3	43.3	255	24.5
	4	47.0	270	25.9
LIFAC Excursion	1	43.0	255	24.5
	2	41.6	260	25.0
	3	41.8	260	25.0
	4	45.3	280	26.9
LIFAC Steady-State	1	43.3	255	24.5
	2	41.9	265	25.4
	3	42.0	260	25.0
	4	46.0	270	25.9

TABLE 7. Tensile Strength of Whitewater Valley Dust Samples

Sample Type	ESP Hopper	Tensile Strength, N/m <sup>2</sup>	
		12% Relative Humidity	23% Relative Humidity
Fly Ash	Inlet	7.5	5.5
Fly Ash	Outlet	32	15
LIFAC Dust	Inlet	9.3	6.8
LIFAC Dust	Outlet	>32	21

**TABLE 8. Whitewater Valley 2 ESP Specifications**

<b>Fields in Direction of Gas Flow</b>	<b>4</b>
<b>Collection Area per Field, ft<sup>2</sup></b>	<b>11,250</b>
<b>Collecting Plate Spacing, in</b>	<b>11</b>
<b>Collecting Plate Height, ft</b>	<b>30</b>
<b>Collecting Plate Length, ft</b>	<b>30</b>
<b>Wire-to-Wire Spacing, in</b>	<b>9</b>
<b>Number of Wires in Flow Direction</b>	<b>40</b>
<b>Number of Gas Passages</b>	<b>25</b>
<b>Number of Baffled Sections</b>	<b>4</b>

TABLE 9a. Whitewater Valley 2 ESP Model Results

	ESP SCA, ft <sup>2</sup> /kacfm	Model Non-Ideal Conditions	Collection Efficiency, %	Particle Emissions, lb/10 <sup>6</sup> Btu	Stack Opacity, %
<b>Model Comparison with Field Data using Standard Non-Ideal Conditions</b>					
Baseline	181	0.05, 0.15	98.76	0.060	13.7
		0.10, 0.25	98.11	0.092	17.8
Water Excursion	195	0.05, 0.15	99.33	0.032	8.6
		0.10, 0.25	98.87	0.053	12.1
LIFAC Excursion	207	0.05, 0.15	99.41	0.052	10.8
		0.10, 0.25	99.00	0.089	15.8
LIFAC Steady-State	207	0.05, 0.15	99.55	0.039	8.4
		0.10, 0.25	99.20	0.069	12.7
<b>LIFAC Model Projections for Various ESP Configurations</b>					
Base ESP	207	0.25, 0.25	97.82	0.188	24.9
		0.50, 0.25	91.06	0.772	57.1
40 ft High Plates	276	0.25, 0.25	98.53	0.127	17.6
		0.50, 0.25	95.59	0.602	49.6
40 ft Plates +1 Field	345	0.25, 0.25	99.38	0.053	8.9
		0.50, 0.25	96.29	0.320	34.6
40 ft Plates +2 Fields	414	0.25, 0.25	99.72	0.024	4.6
		0.50, 0.25	97.88	0.183	23.7

TABLE 9b. Whitewater Valley 2 ESP Model Results

	ESP SCA, ft <sup>2</sup> /kacfm	Model Non-Ideal Conditions	Collection Efficiency, %	Particle Emissions, lb/10 <sup>6</sup> Btu	Stack Opacity, %
<b>Baseline Fly Ash Model Projections for Various ESP Modifications</b>					
40 ft High Plates	241	0.05, 0.15 0.10, 0.25	99.35 98.89	0.032 0.054	8.0 11.2
40 ft Plates +1 Field	302	0.05, 0.15 0.10, 0.25	99.75 99.53	0.012 0.023	3.5 5.5
40 ft Plates +2 Fields	362	0.05, 0.15 0.10, 0.25	99.90 99.79	0.005 0.010	1.6 2.8
<b>High Resistivity Fly Ash Model Projections for Various ESP Modifications</b>					
Base ESP	181	0.05, 0.15 0.10, 0.25	96.59 95.47	0.166 0.220	30.3 34.8
40 ft High Plates	241	0.05, 0.15 0.10, 0.25	97.97 97.12	0.099 0.140	21.1 25.6
40 ft Plates +1 Field	302	0.05, 0.15 0.10, 0.25	99.05 98.56	0.046 0.070	11.9 15.4
40 ft Plates +2 Fields	362	0.05, 0.15 0.10, 0.25	99.53 99.25	0.023 0.037	6.7 9.3

TABLE 10. Whitewater Valley 2 ESP Gas Velocity Profile  
(Gas Velocity in ft/sec)

Dist. from Top	Lane Number											
	2	4	6	8	10	12	14	16	18	20	22	24
1	7.5	6.3	5.0	4.7	6.7	6.2	5.3	4.3	6.0	5.2	5.8	3.2
3	7.3	5.8	4.5	6.2	5.0	5.8	4.7	3.3	5.5	4.5	5.0	4.6
5	6.5	5.2	5.2	5.8	4.7	4.8	4.2	3.2	4.7	4.0	4.2	4.2
7	4.3	5.7	5.8	5.7	3.8	5.0	4.7	3.7	4.7	4.0	4.2	3.7
9	7.1	6.0	4.7	5.8	3.7	5.0	4.5	3.1	4.5	4.2	4.0	4.7
11	7.8	6.0	5.7	7.5	4.5	5.3	4.8	3.7	5.7	5.3	4.7	4.3
13	9.2	6.2	6.5	7.3	5.0	5.5	5.2	5.7	6.2	5.8	4.5	4.5
15	9.2	6.0	7.3	8.7	5.7	7.7	4.8	5.8	6.3	5.8	5.2	5.2
17	10.5	7.0	9.3	9.8	6.7	7.8	6.7	3.7	8.0	8.7	7.0	7.3
19	8.8	9.0	9.0	10.3	7.0	9.8	8.0	5.2	10.0	10.0	8.3	10.0
21	10.7	8.7	7.3	4.8	9.0	15.3	10.0	7.3	7.0	10.5	8.5	9.7
23	13.3	13.0	6.7	1.8	15.0	16.2	15.3	5.7	1.7	16.7	15.3	14.7
25	11.7	13.3	2.5	4.2	15.0	15.7	10.8	6.0	4.8	15.0	11.7	16.0
27	13.7	13.5	12.3	11.7	14.0	12.0	11.2	10.8	10.7	14.0	9.7	12.7
29	1.7	1.6	1.5	1.1	0.9	1.8	1.5	0.2	1.0	0.5	1.7	2.3

Average Velocity, ft/sec = 6.9

**TABLE 11. Modified Whitewater Valley 2 ESP Specifications**

	<b>40 ft High Plates</b>	<b>One Additional Field</b>	<b>Two Additional Fields</b>
<b>Fields in Direction of Gas Flow</b>	<b>4</b>	<b>5</b>	<b>6</b>
<b>Collection Area per Field, ft<sup>2</sup></b>	<b>15,000</b>	<b>15,000</b>	<b>15,000</b>
<b>Collecting Plate Spacing, in</b>	<b>11</b>	<b>11</b>	<b>11</b>
<b>Collecting Plate Height, ft</b>	<b>40</b>	<b>40</b>	<b>40</b>
<b>Collecting Plate Length, ft</b>	<b>30</b>	<b>37.5</b>	<b>45</b>
<b>Wire-to-Wire Spacing, in</b>	<b>9</b>	<b>9</b>	<b>9</b>
<b>Number of Wires in Flow Direction</b>	<b>40</b>	<b>50</b>	<b>60</b>
<b>Number of Gas Passages</b>	<b>25</b>	<b>25</b>	<b>25</b>
<b>Number of Baffled Sections</b>	<b>4</b>	<b>5</b>	<b>6</b>

WHITEWATER VALLEY UNIT 2  
CUMULATIVE MASS SIZE DISTRIBUTION

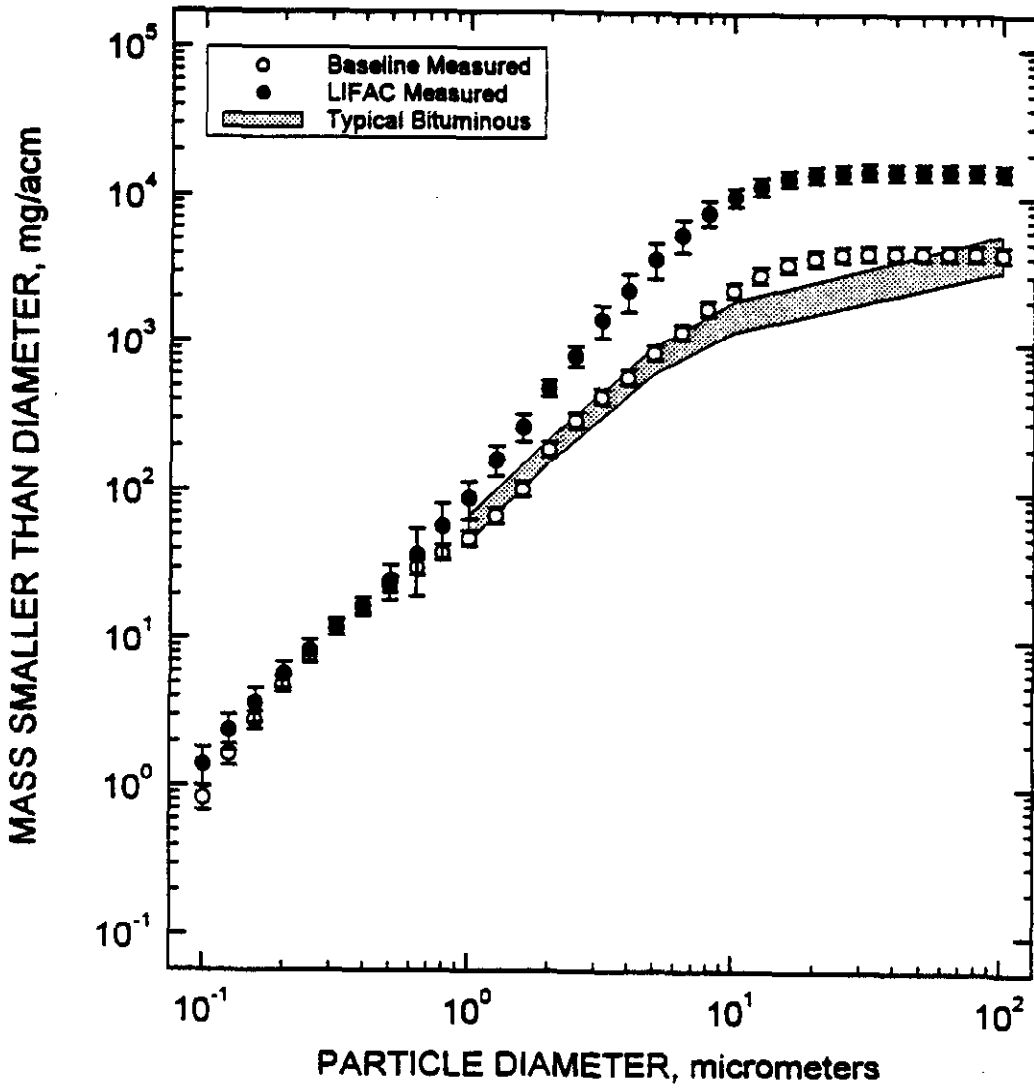


Figure 1. ESP Inlet Cumulative Mass Particle Size Distributions.

### WHITEWATER VALLEY UNIT 2 CUMULATIVE PERCENT SIZE DISTRIBUTION

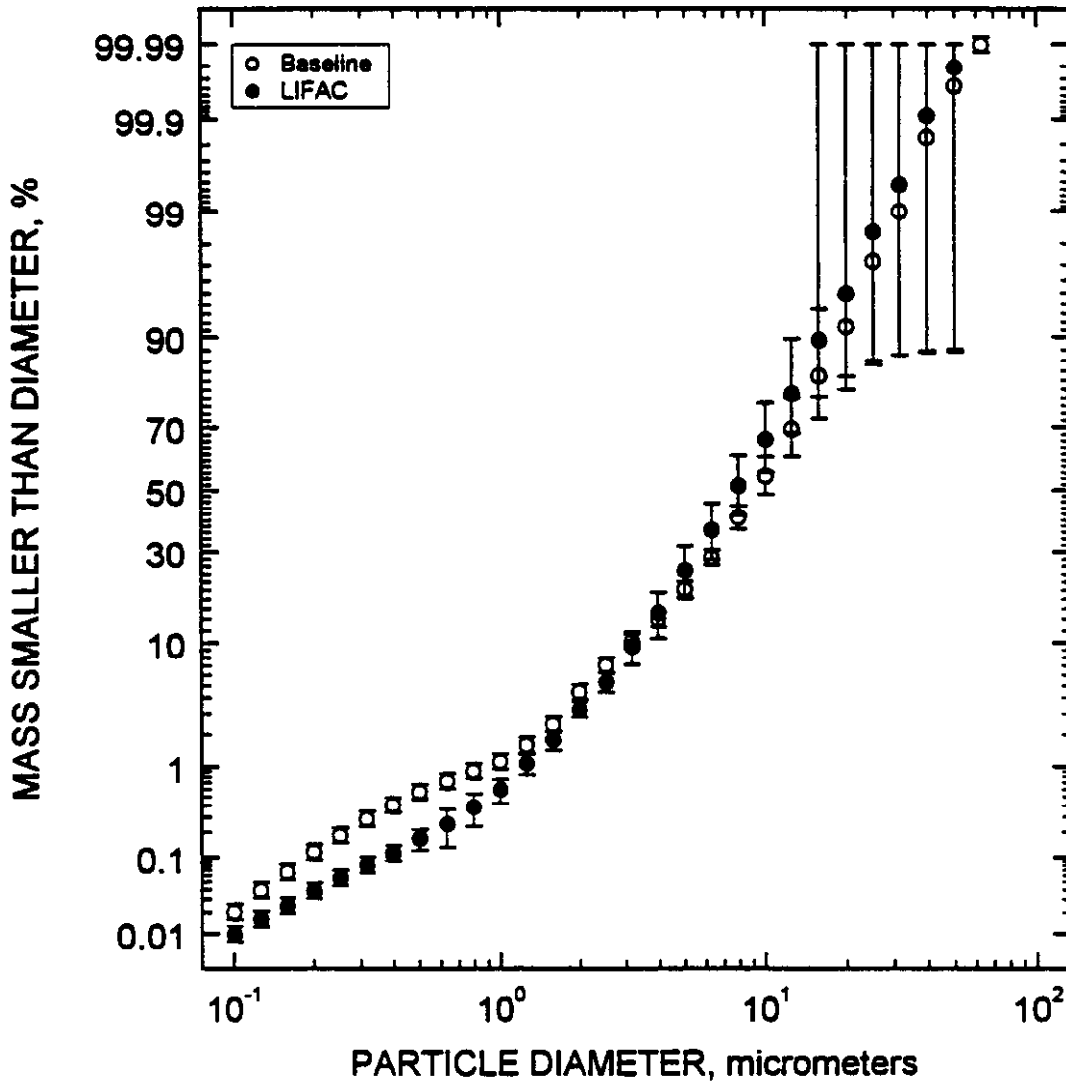


Figure 2. ESP Inlet Cumulative Percent Mass Particle Size Distributions.



MODEL 2 PREDICTED DUST RESISTIVITY  
 WHITEWATER VALLEY FLY ASH

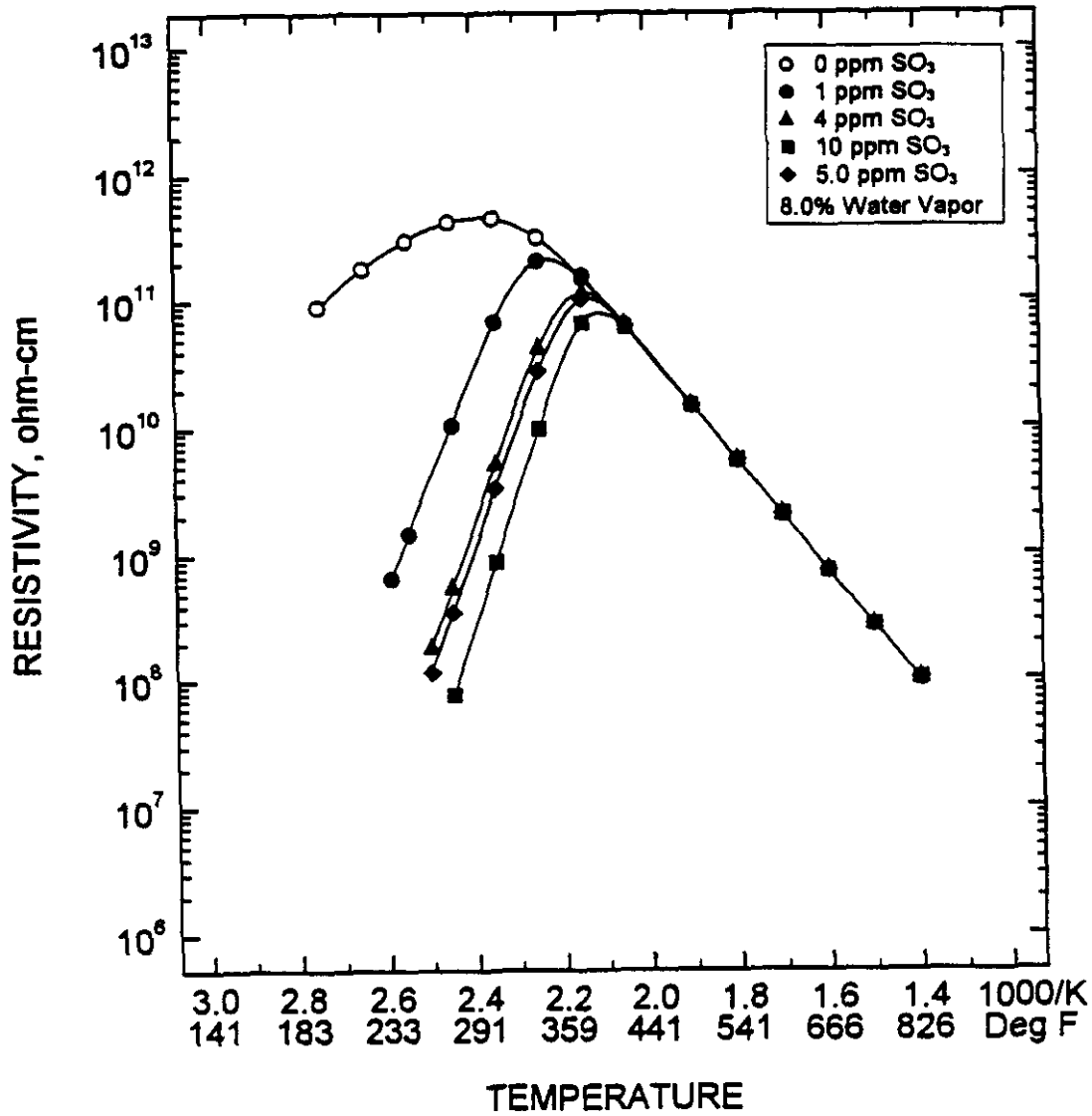


Figure 4. Predicted Resistivity for Baseline Fly Ash.

MODEL 2 PREDICTED DUST RESISTIVITY  
 WHITEWATER VALLEY LIFAC DUST

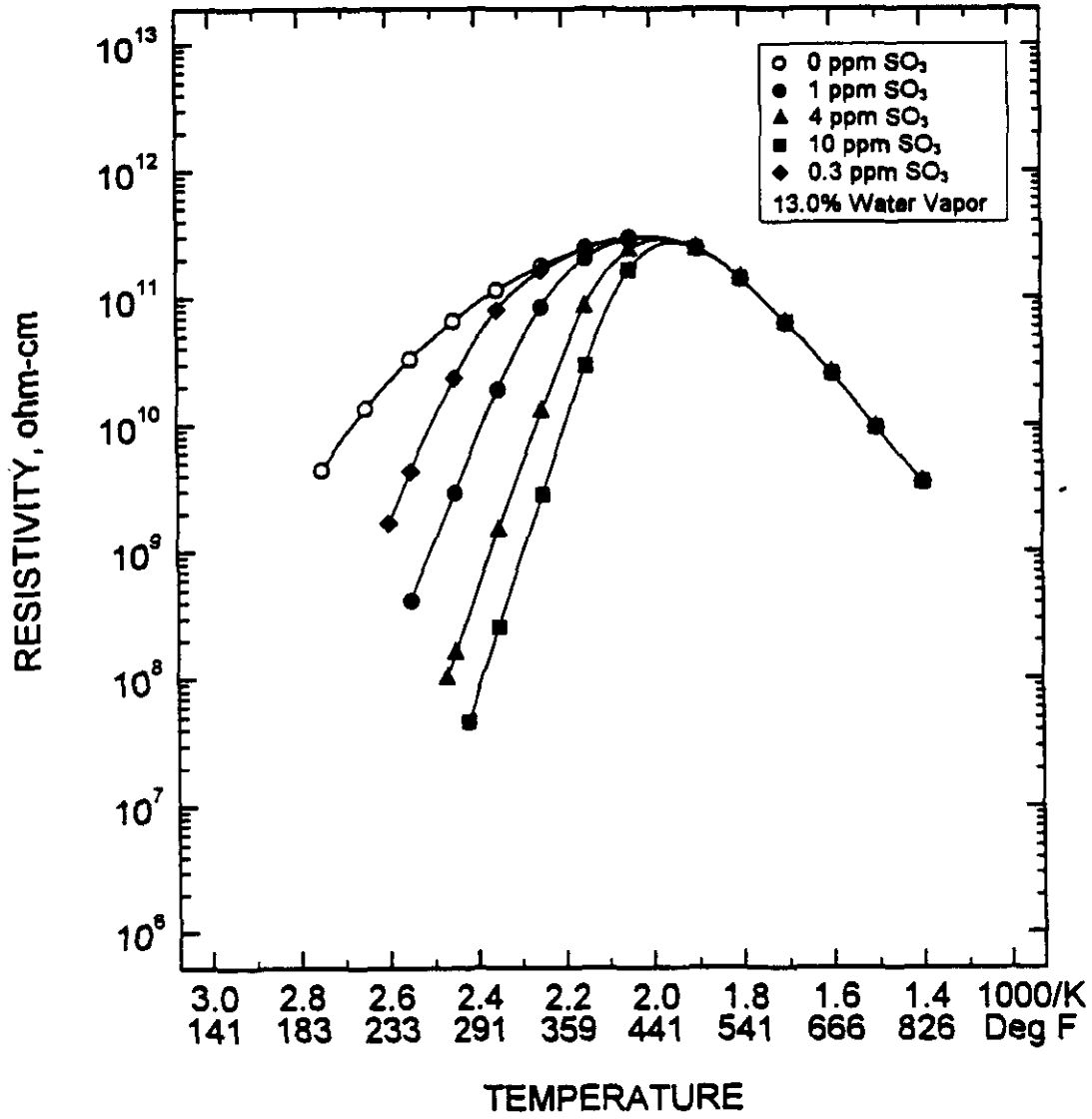


Figure 5. Predicted Resistivity for LIFAC Dust.

### MODELED LIFAC EMISSIONS WITH VARIOUS ESP MODIFICATIONS

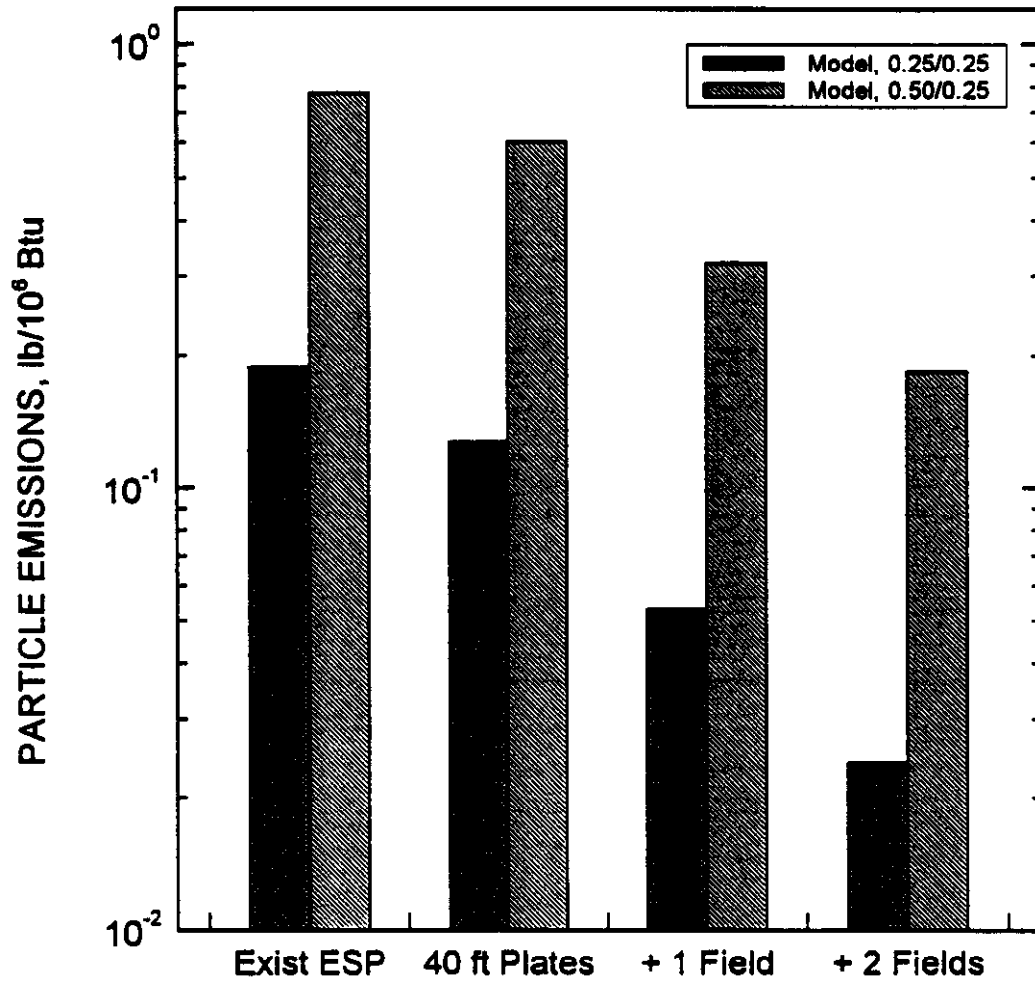


Figure 11. Model Predicted Particle Emissions with LIFAC for Various ESP Modifications.

### MODELED LIFAC OPACITY WITH VARIOUS ESP MODIFICATIONS

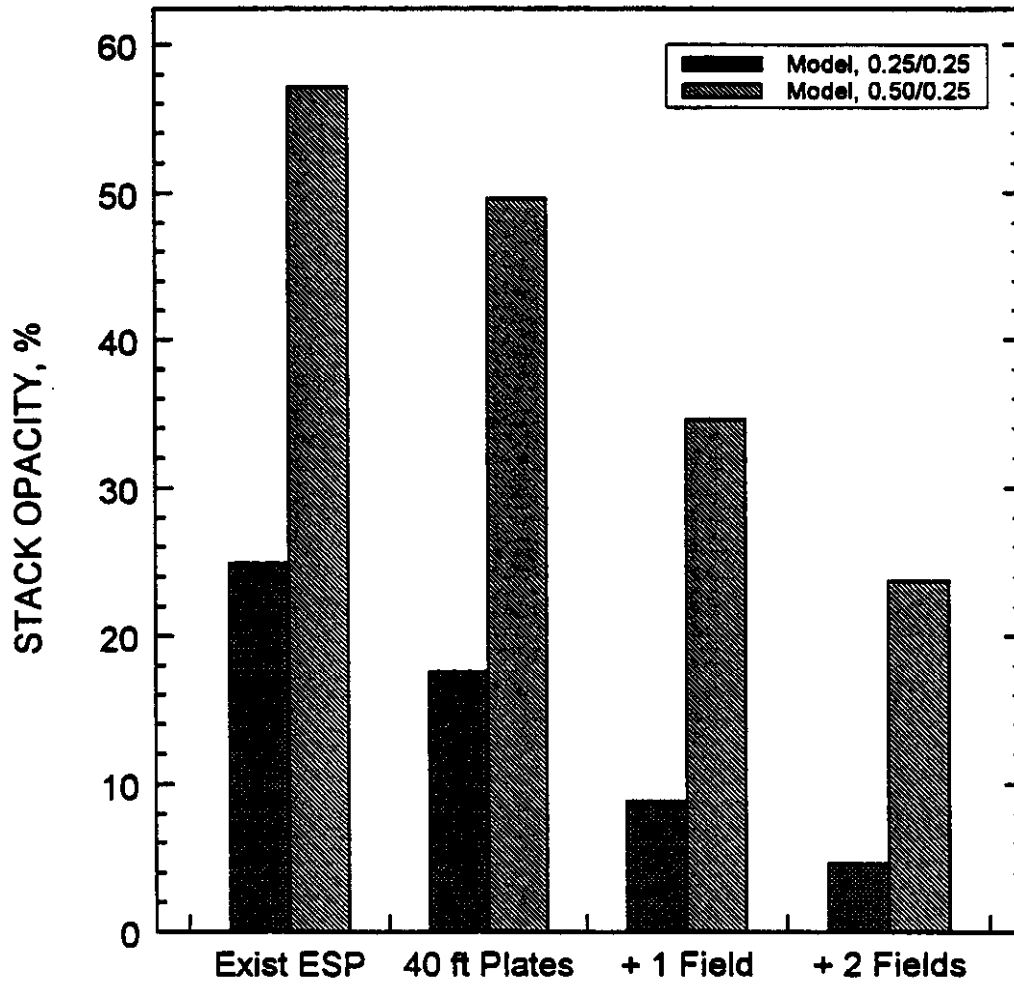


Figure 12. Model Predicted Stack Opacity with LIFAC for Various ESP Modifications.

### MODELED EMISSIONS WITH BASELINE FLYASH FOR VARIOUS ESP MODIFICATIONS

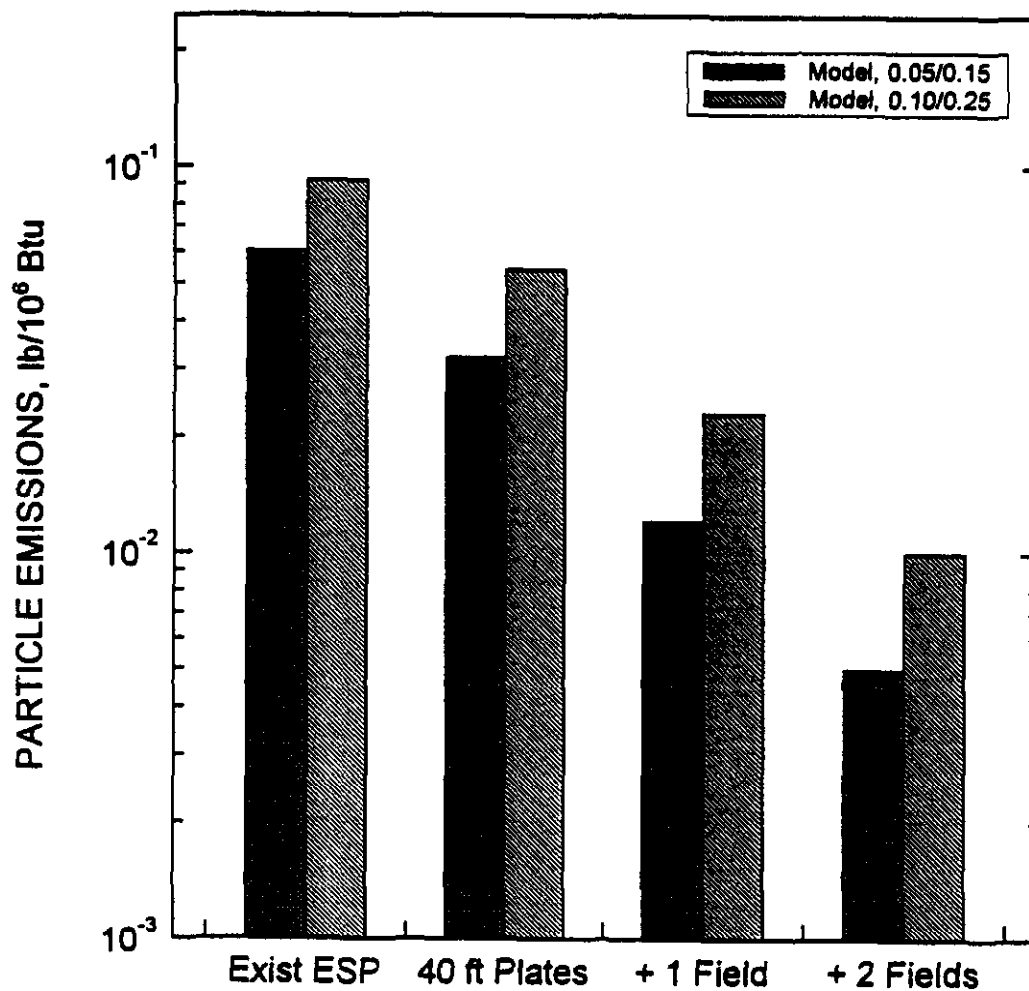


Figure 13. Model Predicted Particle Emissions with Baseline Fly Ash for Various ESP Modifications.

### MODELED OPACITY WITH BASELINE FLYASH FOR VARIOUS ESP MODIFICATIONS

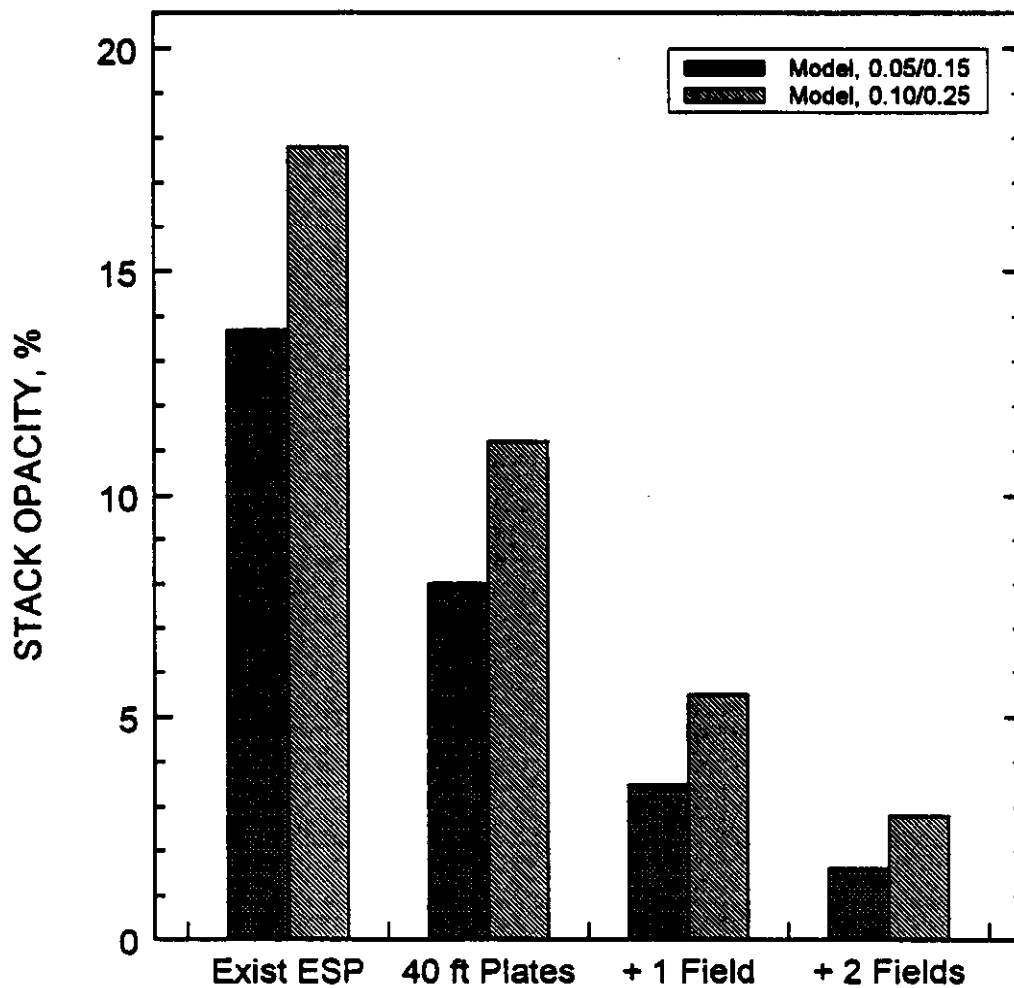


Figure 14. Model Predicted Stack Opacity with Baseline Fly Ash for Various ESP Modifications.

### MODELED EMISSIONS WITH HIGH RESISTIVITY FLY ASH FOR VARIOUS ESP MODIFICATIONS

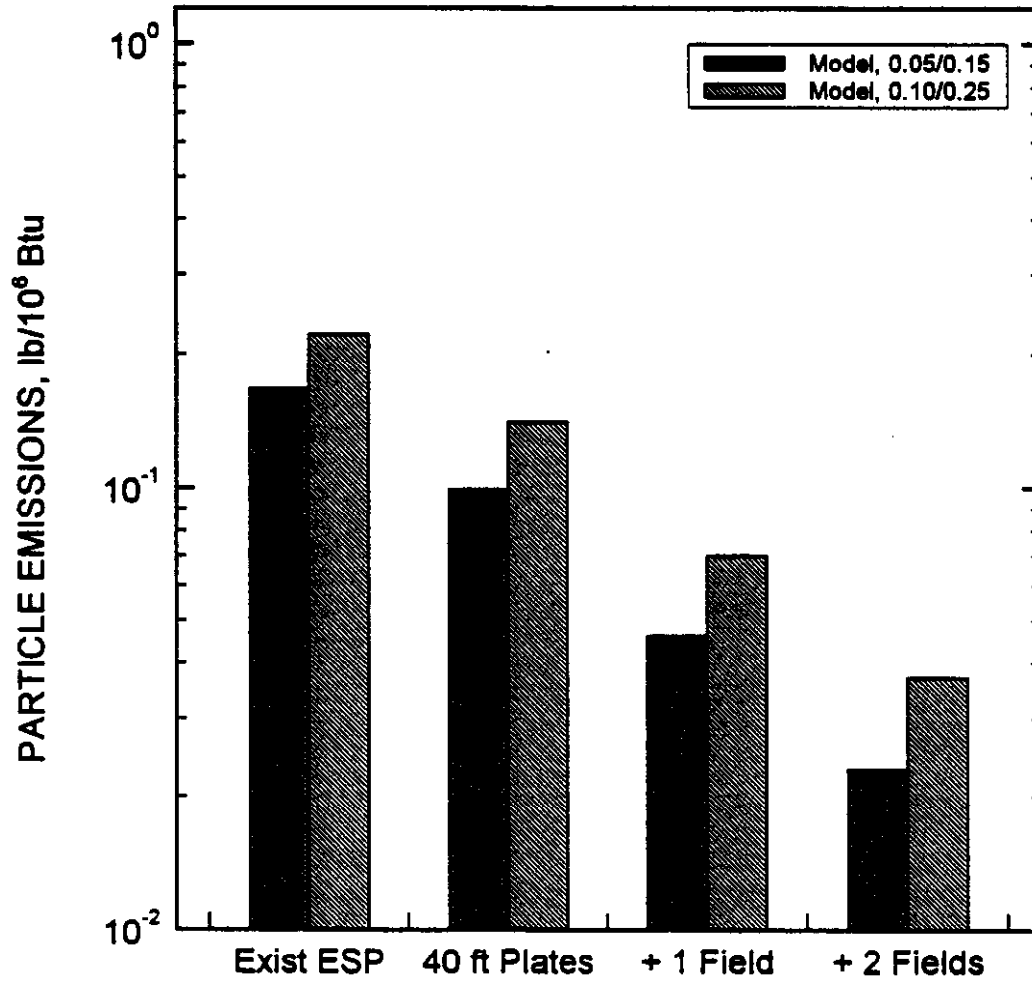


Figure 15. Model Predicted Particle Emissions with High Resistivity Fly Ash for Various ESP Modifications.

### MODELED OPACITY WITH HIGH RESISTIVITY FLY ASH FOR VARIOUS ESP MODIFICATIONS

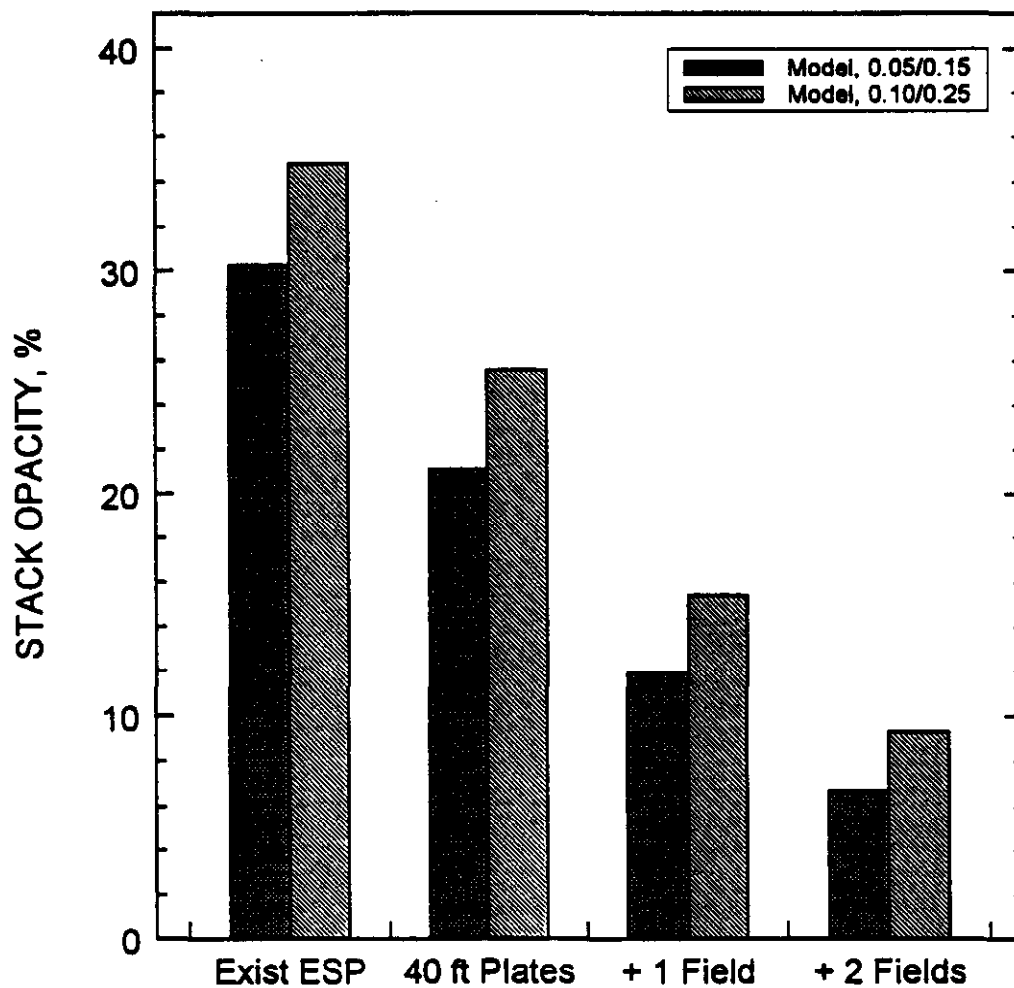


Figure 16. Model Predicted Stack Opacity with High Resistivity Fly Ash for Various ESP Modifications.

### EFFECT OF TEMPERATURE AND MOISTURE CONTENT ON RELATIVE HUMIDITY

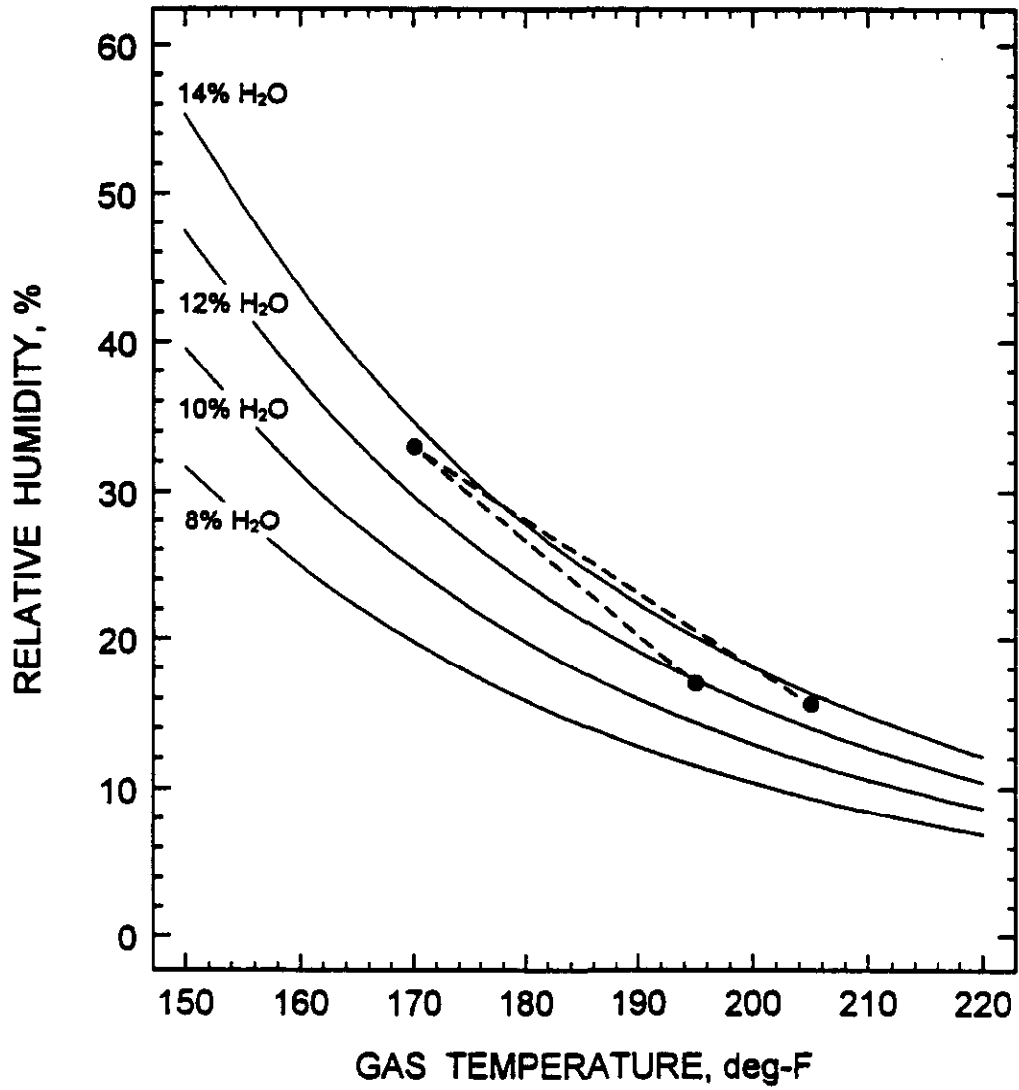


Figure 17. The Effect of Temperature and Moisture Content on Relative Humidity.

